

Detection of insulation defaults in building structures by active infrared thermography

J-L. Bodnar^{*}, A. Szefflinski^{*}, J-C. Candoré^{*}, L. Ibos^{**}, M. Larbi Youcef^{**}, A. Mazioud^{**}, Y. Candau^{**}

^{*}Laboratoire d'Energétique et d'Optique, UFR Sciences Exactes et Naturelles, BP 1039, 51687 Reims cedex 02, France

^{**}CERTES, IUT de Créteil, Université Paris XII, 61 avenue du Général de Gaulle, 94010 Créteil, France

1. Introduction

The detection of insulating defaults in building structures is commonly performed using passive infrared thermography. This method allows detecting insulation defaults in large thermal scenes and with a few thermograms. The main drawback of this method is that a temperature gradient must exist in the wall under study to perform the experiment. On the contrary, active thermography can be used even in the absence of such a temperature gradient. However, this last method is a local method as only a part of a wall can be characterized in one experiment. So, these two methods are complementary techniques for the inspection of building thermal envelope. The objective of this work is to present a method based on active infrared thermography for the detection of thermal insulation defaults of building structures. The insulating structure studied is the most representative of building insulation in France: this structure is composed of two layers, a plaster layer and an expanded polystyrene layer.

2. Experimental

The experimental set-up developed in the Reims university, named SAMMTHIR, is presented in figure 1. This device is based on the excitation of the sample under study by means of two halogen lamps. Infrared thermograms are acquired using a A20 infrared camera from FLIR. A specific electronic device allows synchronising the acquisition of thermograms with the excitation signal.

In this abstract, we will present some of the results obtained on four different samples simulating insulation defaults commonly observed in buildings. For each sample, we present in the same figure, the images of both front and rear sides of the sample, the "photothermal image" obtained by analysis of the thermogram sequence and a 3D representation of this photothermal image. The sample heated by the halogen lamps and observed by the infrared camera is always denoted as the front face. The analysis of the thermogram sequence acquired allows computing the impulse response of the sample for each pixel. The photothermal image is obtained after computing the integral of the impulse response.



Fig. 1. Experimental set-up

3. Results

Figure 2 presents the results obtained on sample A, composed of a plaster layer 1cm thick and of polystyrene layer 6cm-thick. This sample presents two defaults. The first one is a hole of rectangular section performed in the polystyrene layer. The second one simulates the presence of sheath, commonly used for electric cables, inside the polystyrene layer. The photothermal image allows a clear observation of these two defaults.

Sample B, presented in figure 3 is composed of a plaster layer of thickness 13mm and of a polystyrene layer 2cm-thick. In the center of the sample, 1cm of polystyrene was removed. This difference of the insulating layer thickness is clearly visible on the photothermal image of figure 3.

In sample C, the plaster layer thickness is varying continuously from 5mm (in the left part of the sample) to 25mm (in the right part of the sample). The polystyrene layer thickness is also varying as the sample total thickness is equal to 55mm. The photothermal image presented in figure 4 allows observing this continuous variation of the plaster layer thickness.

Finally, sample D simulates the presence of metallic mounting rails ("Placostyle" structure) behind the plaster layer. The position of the rails and of the metallic screws is clearly seen in figure 5.

All examples presented have demonstrated that active infrared thermography is accurate in describing the geometry of the insulating defaults. Thus, this method could be used as a thermal insulation diagnostic tool.

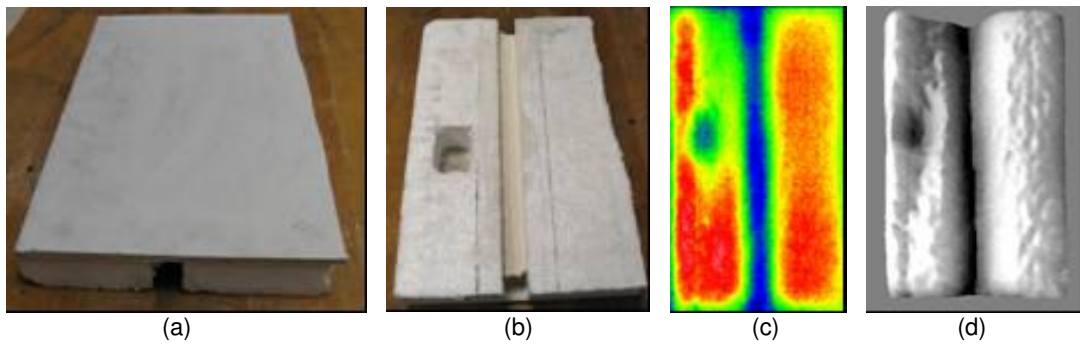


Fig. 2. View of the sample A: (a) front face; (b) rear face; (c) photothermal image obtained; (d) 3D view

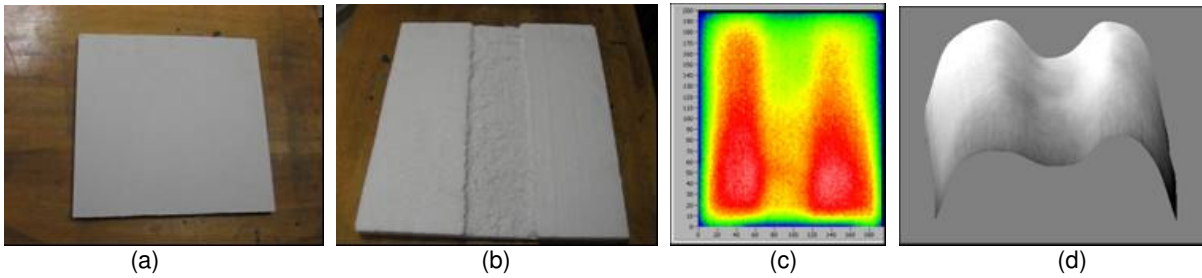


Fig. 3. View of the sample B: (a) front face; (b) rear face; (c) photothermal image obtained; (d) 3D view

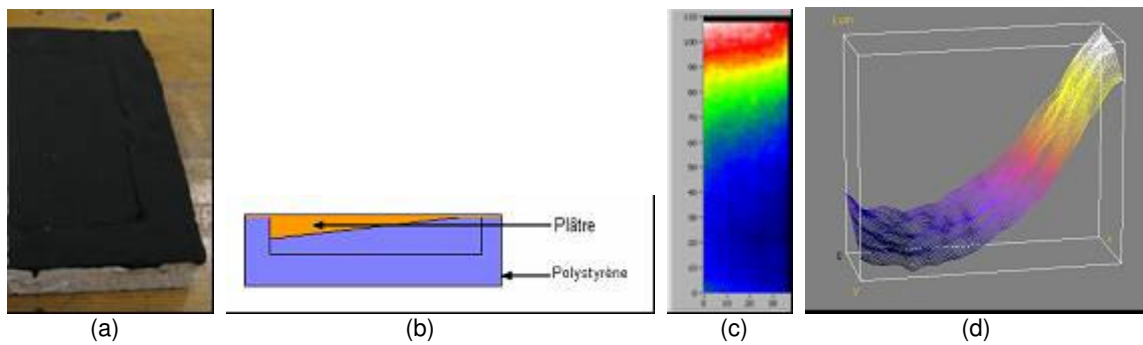


Fig. 4. View of the sample C: (a) front face; (b) rear face; (c) photothermal image obtained; (d) 3D view

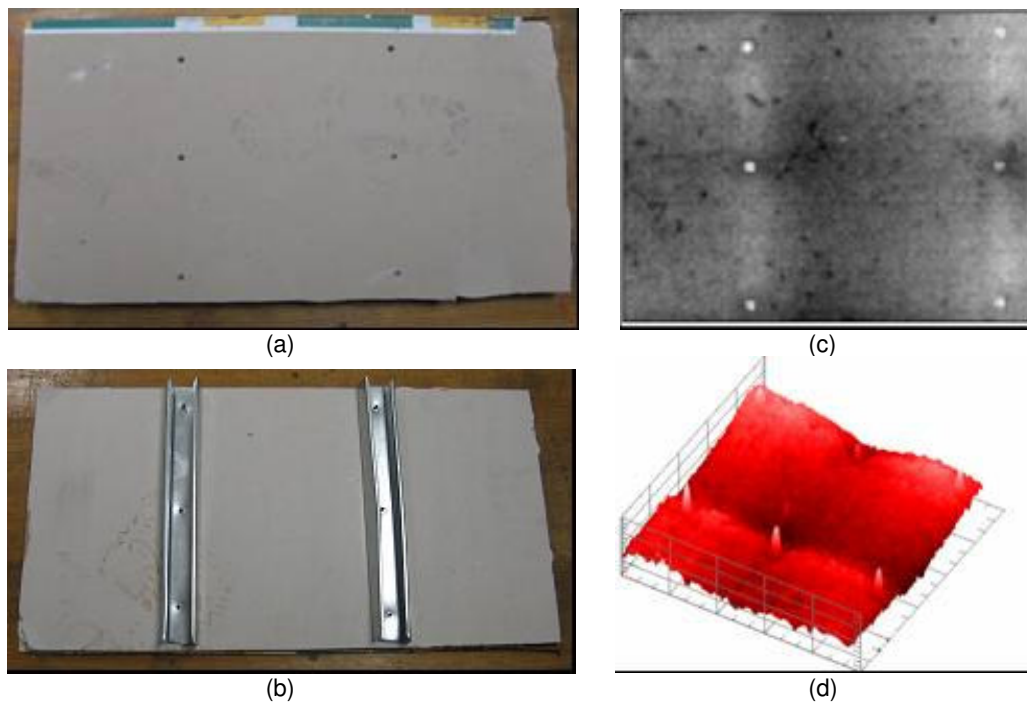


Fig. 5. View of the sample D: (a) front face; (b) rear face; (c) photothermal image obtained; (d) 3D view